Tilted dipole bands in ^{123,124}Xe

G. Rainovski,[1,*] D. L. Balabanski,[1] G. Roussev,[1] G. Lo Bianco,[2,3] G. Falconi,[2] N. Blasi,[3] D. Bazzacco,[4] G. de Angelis,[5] D. R. Napoli,[5] F. Dönau,[6] and V. I. Dimitrov[1]
[1]*St. Kliment Ohridski University of Sofia, BG-1164 Sofia, Bulgaria*
[2]*Universita Di Camerino, I-62032 Camerino, Italy*
[3]*INFN-Sezione Di Milano, I-20133 Milano, Italy*
[4]*INFN-Sezione Di Padova, I-35131 Padova, Italy*
[5]*INFN-Laboratori Nazionali Di Legnaro, I-35020 Legnaro, Italy*
[6]*Forschungszentrum Rossendorf, D-01314 Dresden, Germany*

(Received 28 February 2001; revised manuscript received 1 May 2002; published 18 July 2002)

High-spin states in ^{123}Xe were populated in the ^{110}Pd(^{18}O,5n) reaction at 75 MeV and gamma-ray coincidences were measured with the GASP spectrometer. A new rotational sequence of enhanced dipole transitions was established. This band, as well as a similar band in ^{124}Xe, may be described within the framework of the tilted axis cranking model as bands for which comparable amounts of angular momentum are generated by magnetic and collective rotation, respectively.

DOI: 10.1103/PhysRevC.66.014308 PACS number(s): 21.10.Re, 21.60.Ev, 27.60.+j

I. INTRODUCTION

Magnetic rotation in atomic nuclei has attracted significant experimental and theoretical interest in the last few years. It occurs in weakly deformed (nearly spherical) nuclei and is characterized by the appearance of regular sequences of enhanced $M1$ transitions. Frauendorf developed the concept of magnetic rotation in order to describe these bands [1,2] and examples of this mode of excitation have been found in different mass regions [3]. The magnetic bands are described within the framework of the tilted axis cranking (TAC) model [4,5]. A simplified description of magnetic rotation can be given as follows: the currents of a small number of valence high-j particles and high-j holes tend to be oriented perpendicularly to each other in a nearly spherical nucleus to form a magnetic dipole. As a result, their angular momenta $\vec{j}_\pi$ and $\vec{j}_\nu$ (here π and ν indicate protons and neutrons, respectively) couple to a total nuclear angular momentum vector $\vec{I}$, which is tilted with respect to the principal axes of the nucleus. This kind of coupling causes a spontaneous breaking of the signature symmetry with respect to the intrinsic frame, which leads to the appearance of $\Delta I = 1$ sequences [6]. The total angular momentum is increased by the gradual alignment of $\vec{j}_\pi$ and $\vec{j}_\nu$ along the rotational axis, a process which is named the "shears" mechanism. The magnetic moment has a large transverse component $\mu_\perp$, which gives rise to enhanced $M1$ transitions in the shears band.

An interesting question is whether the shears mechanism can also exist in deformed nuclei in which angular momentum is usually generated by collective rotation. In other words, where are the boundaries of the phenomenon of magnetic rotation and what is the interplay between the shears mechanism and collective rotation? The $_{54}$Xe and $_{56}$Ba nuclei in the $A \approx 120$–130 mass region have a moderate quadrupole deformation of $\epsilon_2 \approx 0.2$ and are expected to be good candidates for such studies. Several $\Delta I = 1$ bands of enhanced $M1$ transitions with no signature splitting have been observed in the even-even $_{56}$Ba [7–9] and $_{54}$Xe [10–13] nuclei. These bands appear at excitation energies of about 4 MeV and 5 MeV for the Ba and the Xe isotopes, respectively. The lowest observed state in most of these bands has spin $I \approx 12\ \hbar$ [9,12,13] and it has been proposed that the bands have four-quasiparticle configurations containing a $\pi h_{11/2}$ particle and a $\nu h_{11/2}$ hole. They have been described in the framework of the geometrical model of Dönau and Frauendorf [14] as high-K multi-quasi-particle bands [9,12,13]. However, this is a semiclassical description and cannot account fully for the properties of the nuclear system. Recent lifetime measurements provide evidence that a more sophisticated approach is necessary to describe the dipole band in ^{128}Ba [15]. A self-consistent description of this band has been proposed within the framework of the hybrid TAC model [16] where it is understood as a magnetic band of intermediate character for which comparable amounts of angular momentum are generated by the shears mechanism and by collective rotation. This conclusion was based on the calculated dependence of the tilt angle on the rotational frequency—$\Theta(\omega)$ [16]. The proposed intermediate picture is logical, because nuclei in the Xe-Ba region are much more deformed than the nuclei in the vicinity of closed shells, where magnetic rotational bands have been observed to date [2].

In this paper we report on a new dipole band observed in the odd-A nucleus ^{123}Xe. This band, as well as a similar band which was observed in the neighboring even-even ^{124}Xe [11,12], are described as dipole bands of intermediate nature.

II. EXPERIMENTAL METHODS AND RESULTS

High-spin states in ^{123}Xe were populated in the reaction ^{110}Pd(^{18}O,5n) at 75 MeV. The ^{18}O beam, which was provided by the XTU tandem accelerator at the Legnaro National Laboratory, was incident on an enriched 10 mg/cm^2 ^{110}Pd target. The nuclear γ decay was studied with the GASP spectrometer [17]. A total of 4.5×10^9 coincidence

*Present address: Oliver Lodge Laboratory, University of Liverpool, Liverpool L69 7ZE, United Kingdom.

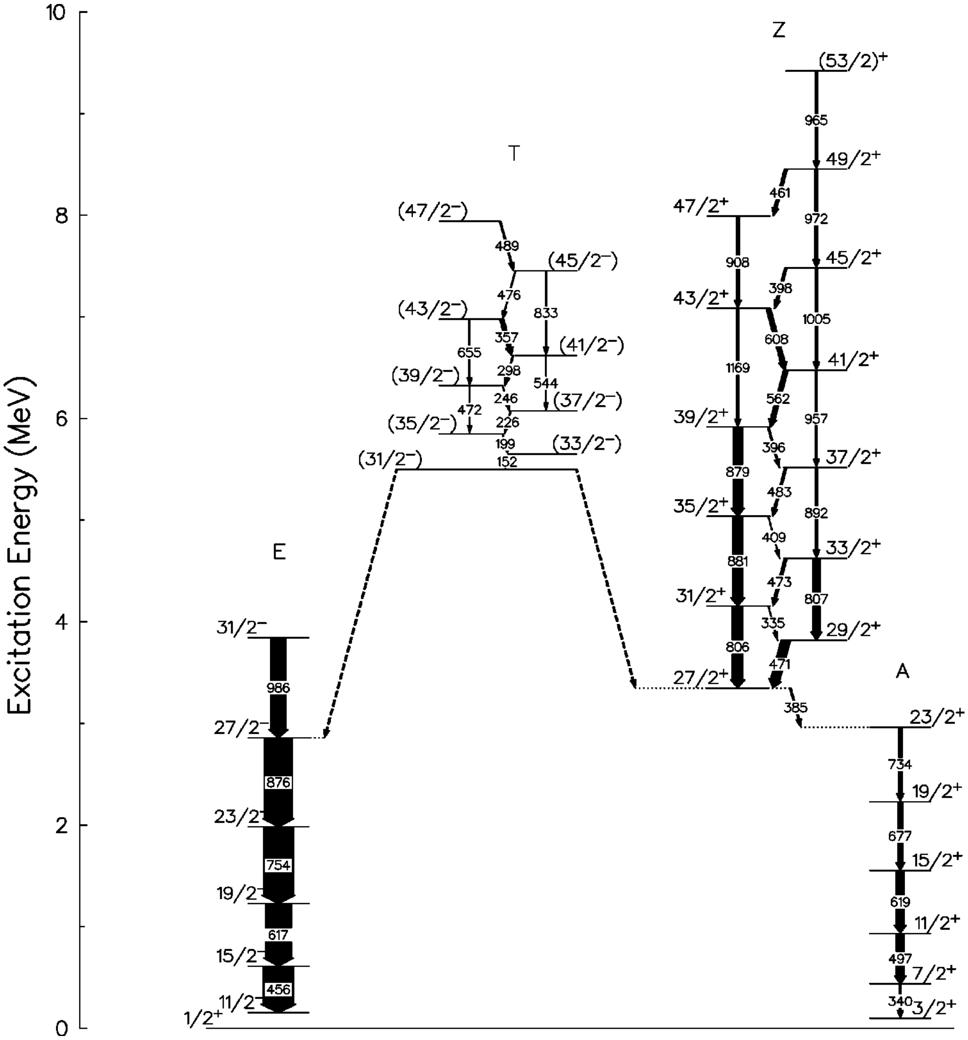

FIG. 1. Partial level scheme of ^{123}Xe showing the new dipole band T and the bands to which it decays. Tentative spins are in parentheses. The thickness of the arrows is proportional to the γ-ray intensity.

events, which satisfied the condition of at least three HPGe and three BGO detectors firing, were accumulated during the experiment. The data were sorted into $\gamma\gamma$ matrices and the level scheme of ^{123}Xe was constructed using coincidence relationships and the relative intensities of γ-ray transitions.

To deduce multipole orders of γ rays, directional correlation (DCO) ratios [18,19] were analyzed. γ-γ events with one γ ray detected in one of the 12 detectors placed at 31.7° and 36.0° (average 35°), at the complementary angles 144.0° and 148.3° (average 145°), and the other γ ray detected in one of the eight detectors at 90° relative to the beam direction were sorted into a coincidence matrix. Coincidence spectra were extracted from the (35°,90°) and the transposed (90°,35°) matrices. The DCO ratios were obtained as the ratios of γ-ray transition intensities in both background-corrected spectra. A DCO ratio of 1.0 is expected if the gating and observed transitions are stretched transitions of pure and equal multipole order. For the present detector geometry, a value of 0.54 is expected for a pure dipole transition gated on a stretched quadrupole transition.

High-spin states in ^{123}Xe have been studied recently by Schmidt *et al.* [20]. In our work we confirm most of the transitions that were reported in Ref. [20] and, in addition, we established a new band. This band (denoted T) is shown in Fig. 1 and the γ rays assigned to band T are listed in Table I. A sample spectrum, revealing the transitions in band T, is shown in Fig. 2. The order of the levels is unambiguously fixed by the weak crossover transitions. Whenever they could be reliably determined, the DCO ratios were found to be consistent with $M1$ multipolarity for the cascade transitions.

Low-lying transitions in bands A and E (as shown in Fig. 1) were observed in coincidence with band T. The highest placed transitions which are in coincidence with band T are the 876 keV γ ray, which belongs to band E, and the 385 keV transition, which connects band Z with band A (see Fig. 1). Both transitions depopulate $I=\frac{27}{2}$ states [20]. The decay of band T is probably fragmented into several paths, since the linking transitions to the $I=\frac{27}{2}$ states were not observed. Possible values for the bandhead spin are $I=(\frac{29}{2})$ and $I=(\frac{31}{2})$. Taking into account the relative population of band T with respect to the other bands in the scheme of ^{123}Xe (Fig. 1), its bandhead should be placed at about 5.5 MeV.

The $\nu h_{11/2}$ configuration has been proposed in Ref. [20] for band E, which is in agreement with the systematics in the region. Band A has the $\nu d_{3/2}$ configuration and the $\nu[h_{11/2}^2 g_{7/2}]$ configuration has been suggested for band Z

TABLE I. Energies, intensities, DCO ratios, and multipolarities for the transitions belonging to band T in ^{123}Xe, as obtained in the present work.

$I_i \rightarrow I_f$	E_γ [a] [keV]	I_γ [b]	DCO ratio [c]	Multipolarity [d]
$(\frac{33}{2}^-) \rightarrow (\frac{31}{2}^-)$	152.0	4.4 ± 0.4	0.4 ± 0.2	$M1$
$(\frac{35}{2}^-) \rightarrow (\frac{33}{2}^-)$	199.3	2.8 ± 0.2		$(M1)$
$(\frac{37}{2}^-) \rightarrow (\frac{35}{2}^-)$	226.1	3.3 ± 0.3		$(M1)$
$(\frac{39}{2}^-) \rightarrow (\frac{37}{2}^-)$	245.5	2.8 ± 0.2		$(M1)$
$(\frac{39}{2}^-) \rightarrow (\frac{35}{2}^-)$	471.8	0.20 ± 0.05 [e]		$(E2)$
$(\frac{41}{2}^-) \rightarrow (\frac{39}{2}^-)$	298.2	3.8 ± 0.3	0.6 ± 0.2	$M1$
$(\frac{41}{2}^-) \rightarrow (\frac{37}{2}^-)$	544.1	0.7 ± 0.2 [e]		$(E2)$
$(\frac{43}{2}^-) \rightarrow (\frac{41}{2}^-)$	357.4	13.1 ± 0.9	0.5 ± 0.2	$M1$
$(\frac{43}{2}^-) \rightarrow (\frac{39}{2}^-)$	655.2	2.7 ± 0.5 [e]		$(E2)$
$(\frac{45}{2}^-) \rightarrow (\frac{43}{2}^-)$	475.7	2.6 ± 0.3		$(M1)$
$(\frac{45}{2}^-) \rightarrow (\frac{41}{2}^-)$	833.2	3.7 ± 0.6 [e]		$(E2)$
$(\frac{47}{2}^-) \rightarrow (\frac{45}{2}^-)$	489.3	4.8 ± 0.9	0.7 ± 0.2	$(M1)$

[a]The errors in the transition energies are between 0.1 and 0.4 keV.
[b]The intensities were obtained from the full projection and normalized to the intensity of the 456.3 keV transition $(\frac{15}{2}^- \rightarrow \frac{11}{2}^-)$.
[c]DCO ratios determined in summed γ-ray coincidence spectra produced by gating on all $E2$ transitions of bands A and E which are in coincidence with band T.
[d]Multipolarity compatible with the DCO ratio and the deexcitation mode.
[e]The intensity of this transition was obtained in a coincidence spectrum gated on the $M1$ transition which directly populates the level of interest.

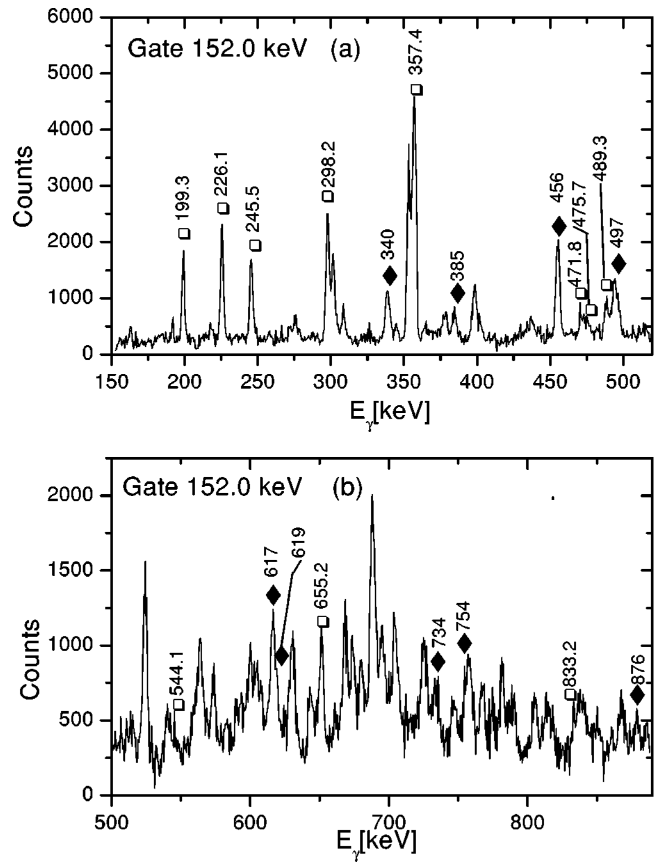

FIG. 2. Coincidence spectrum gated on the 152.0 keV transition of the band T. The transitions which belong to band T are denoted by open squares and those of bands A and E are marked with filled diamonds.

[20]. Band T in ^{123}Xe is most likely a five-quasiparticle band. The alignment vs rotational frequency of the dipole bands in ^{123,124}Xe is displayed in Fig. 3. Both bands have a similar behavior in the frequency interval for which band T was observed. The initial alignment of band T is about $3\hbar$ larger than the initial alignment of the dipole band in ^{124}Xe. The difference between the initial alignments can be explained with an extra $\nu h_{11/2}$ particle which is present in the structure of band T. The initial alignment of the $\nu h_{11/2}$ particles is approximately $3\hbar$, as shown in Fig. 3, while the $\nu d_{3/2}$ particles, which can also be considered in the configuration of band T, have zero initial alignment.

From this experiment we were able to deduce the ratios of reduced transition probabilities for four states of band T in ^{123}Xe. We assume a pure $M1$ character for the $\Delta I=1$ transitions (i.e., $\delta=0$). The last assumption is based on the measured mixing ratios for the dipole band in ^{124}Xe [12]. They are relatively small (0.14–0.17) [12] and cannot influence the results for $B(M1)/B(E2)$ ratios by more than 2%.

III. TILTED AXIS CRANKING MODEL CALCULATIONS

The dipole band in ^{124}Xe is a four-quasiparticle band with a suggested $\pi[h_{11/2}(d_{5/2}/g_{7/2})]\otimes\nu[h_{11/2}(d_{5/2}/g_{7/2})]$ configuration [12]. Assuming prolate deformation, the $h_{11/2}$ proton occupies the $\Omega=\frac{1}{2}$ Nilsson state, the $h_{11/2}$ neutron is in the $\Omega=\frac{7}{2}$ Nilsson state, and the $d_{3/2}$ particles occupy the $\Omega=\frac{3}{2}$ states. Note that the $d_{5/2}$ and the $g_{7/2}$ particles are strongly mixed for both protons and neutrons. By adjusting several parameters, the K value, the intrinsic quadrupole moment, Q_0, and the difference of the gyromagnetic factors $|(g_K-g_R)|$, Schneider *et al.* were able to describe the $B(M1)/B(E2)$ ratios in the four-quasiparticle band in ^{124}Xe [12], using the geometrical model of Dönau and Frauendorf [14].

We have chosen a different approach for the description of the dipole bands in the Xe nuclei. The $B(M1)/B(E2)$ ratios for the dipole bands in ^{123,124}Xe were compared to calculations within the hybrid TAC model [16]. The hybrid TAC model is a version of the TAC model, in which the Nilsson potential is adjusted to be as close as possible to a Woods-Saxon shape. This is done, as described in Ref. [16], by using the energies of the spherical Woods-Saxon potential plus a deformed part which is an anisotropic harmonic oscillator. It is well known that the Woods-Saxon potential with the universal set of parameters [21] is a better approximation for mass $A\approx130$ nuclei [22]. This is a reasonable approximation as long as the deformation is moderate, which is the case for ^{123,124}Xe.

The present TAC model calculations are self-consistent with respect to the deformation parameters only. The pairing

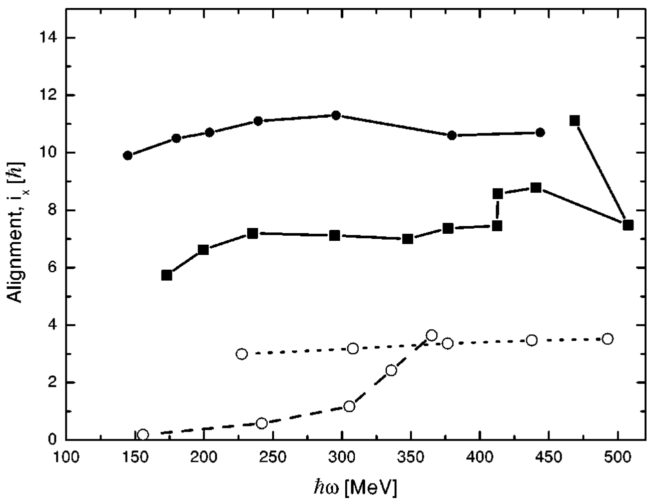

FIG. 3. Alignment plots for the rotational bands in ^{123}Xe: band T (solid line, filled circles), the $\nu d_{3/2}$ band (band A in Fig. 1) (dashed line, open circles), and the $\nu h_{11/2}$ band (band E in Fig. 1) (dotted line, open circles), compared with the dipole band in ^{124}Xe (solid line, filled squares). The Harris parameters used were $\mathcal{J}^0 = 16$ MeV$^{-1}\hbar^2$, $\mathcal{J}_1 = 30$ MeV$^{-3}\hbar^4$.

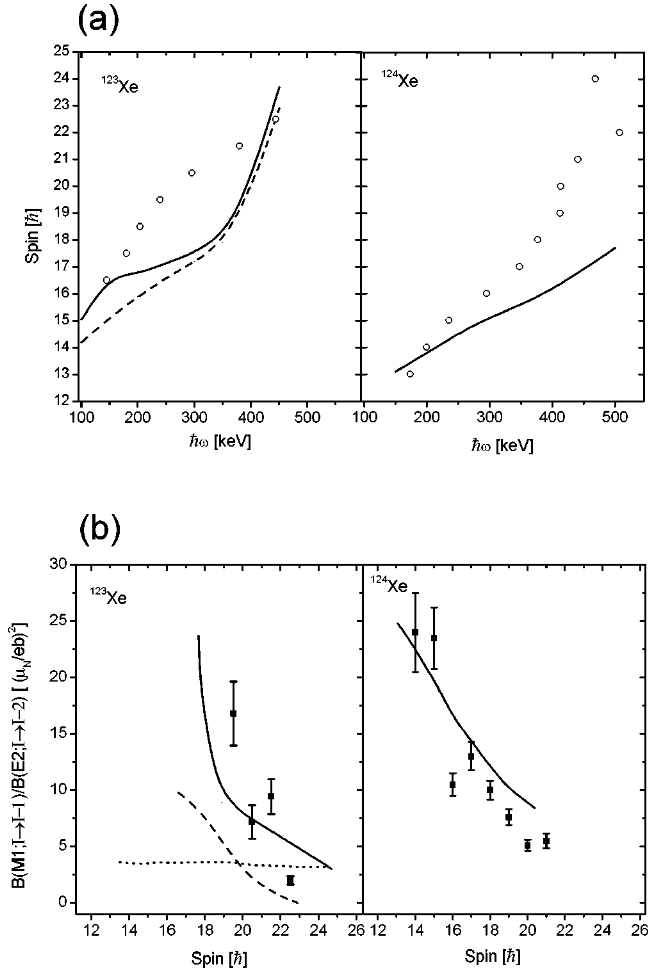

FIG. 4. Comparison of the experimental observables in the dipole bands in ^{123,124}Xe to theoretical calculations. (a) Experimental spins (open circles): in the left-hand side of the figure TAC model predictions for the $\pi[h_{11/2}(d_{5/2}/g_{7/2})]\otimes\nu[h_{11/2}(d_{5/2}/g_{7/2})d_{3/2}]$ (dashed line) and the $\pi[h_{11/2}(d_{5/2}/g_{7/2})]\otimes\nu[h^2_{11/2}(d_{5/2}/g_{7/2})]$ (solid line) configurations in ^{123}Xe at $\epsilon_2\approx 0.20, \gamma\approx 29°$ and in the right-hand side for the $\pi[h_{11/2}(d_{5/2}/g_{7/2})]\otimes\nu[h_{11/2}(d_{5/2}/g_{7/2})]$ (solid line) configuration in ^{124}Xe at $\epsilon_2\approx 0.19, \gamma\approx 30°$ are presented; (b) experimental $B(M1)/B(E2)$ ratios in ^{123,124}Xe are compared to TAC model predictions for the above configurations at the same deformations (the same notations are used). In the left-hand side of the figure a calculation within the geometrical model for the $\pi[h_{11/2}d_{5/2}]\otimes\nu[h^2_{11/2}g_{7/2}]$ configuration at prolate deformation, $\epsilon_2 = 0.2$, is displayed (dotted line).

properties are fixed by the pairing field, which is determined in the TAC model by the gap parameter Δ (for more details see Ref. [6]). Since a large reduction of the pairing gap can be expected for multi-quasi-particle excitations in our calculations we used the following gap parameters: $\Delta_\nu = 0.77$ MeV for neutrons and $\Delta_\pi = 1.0$ MeV for protons, which correspond to about 75% of the experimental even-odd mass difference.

The lowest-lying $4qp$ positive parity state in ^{124}Xe, according to the calculations, has the $\pi[h_{11/2}(d_{5/2}/g_{7/2})]\otimes\nu[h_{11/2}(d_{5/2}/g_{7/2})]$ configuration at an equilibrium deformation $\epsilon_2\approx 0.19$, $\gamma\approx 30°$. Both the angular momentum vs the rotational frequency, $I(\hbar\omega)$ [Fig. 4(a)], and the ratios of the reduced transition probabilities [Fig. 4(b)] were calculated for this configuration.

The calculations reproduce the increasing trend of the angular momentum vs the rotational frequency. However, at high frequencies the discrepancy with the experiment reaches a factor of 2 [see Fig. 4(a)]. Similar discrepancy is observed also in the case of ^{123}Xe. The reason is that the moment-of-inertia parameters are only poorly reproduced in the calculations. It is known that these parameters are quite sensitive to the pairing properties. In the present calculation standard values for the pairing gaps were taken, as derived from the binding energies. By fine tuning the pairing gaps, the agreement could be improved. On the other hand, effects such as quadrupole pairing are not included in the TAC mean field at present. Such effects might be the reason for the above discrepancy, because the ^{123,124}Xe nuclei are known to have a moderate deformation.

For the $B(M1)/B(E2)$ ratios the trend and the magnitude are reproduced [Fig. 4(b)] by the calculations. The solution obtained is a tilted one. The tilt angle takes values of about 60° and slightly increases within the frequency region in which the band is observed [Fig. 5(a)]. This is an indication that the shears mechanism has a significant contribution to the total angular momentum. However, it is not the shears mechanism alone, which is responsible for building up the angular momentum in the band. The core has a significant deformation which favors collective rotation as well. Thus, we consider the dipole band in ^{124}Xe to be of intermediate character.

The TAC calculations for the band T in ^{123}Xe yield that the lowest-lying $5qp$ configurations of opposite parity are the $\pi[h_{11/2}(d_{5/2}/g_{7/2})]\otimes\nu[h_{11/2}(d_{5/2}/g_{7/2})d_{3/2}]$ and the $\pi[h_{11/2}(d_{5/2}/g_{7/2})]\otimes\nu[h^2_{11/2}(d_{5/2}/g_{7/2})]$ at the same equilibrium deformation $\epsilon_2\approx 0.20$, $\gamma\approx 29°$.

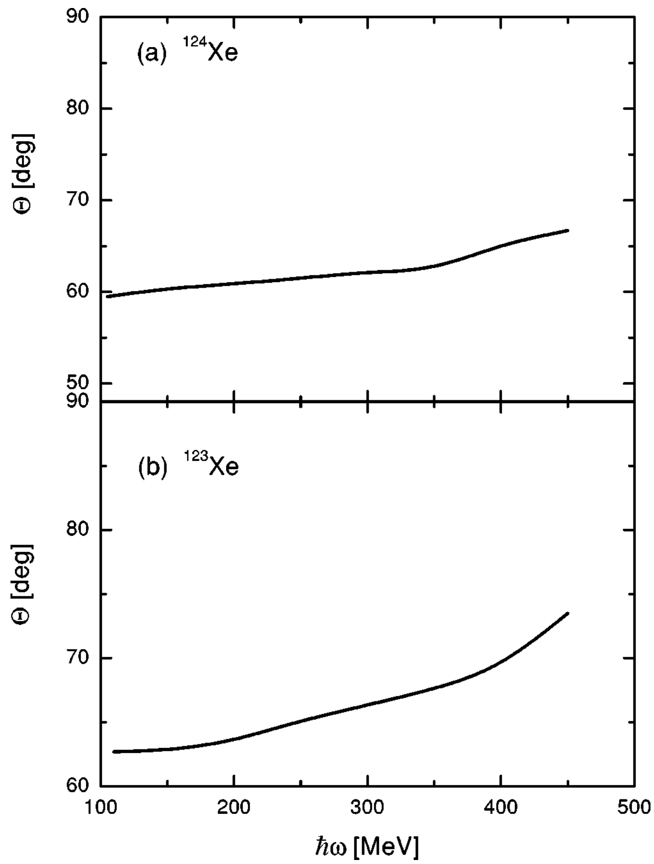

FIG. 5. The dependence of the tilt angle vs the rotational frequency: (a) for the $\pi[h_{11/2}(d_{5/2}/g_{7/2})]\otimes\nu[h_{11/2}(d_{5/2}/g_{7/2})]$ configuration in ^{124}Xe at $\epsilon_2\approx0.19,\gamma\approx30°$; (b) for the $\pi[h_{11/2}(d_{5/2}/g_{7/2})]\otimes\nu[h^2_{11/2}(d_{5/2}/g_{7/2})]$ configurations in ^{123}Xe at $\epsilon_2\approx0.20,\gamma\approx29°$.

The calculated dependencies of the spin vs the rotational frequency are shown in Fig. 4(a). For both configurations, as in the case of ^{124}Xe, there is discrepancy between experimental values and the calculations at high frequencies. The calculated $I(\hbar\omega)$ function for the latter configuration is closer to the experimental values at low rotational frequencies and like the former one bend up at higher frequencies [Fig. 4(a)]. This behavior is quite similar to the one observed in the paired calculation for the tilted band in ^{128}Ba [6] but the bigger discrepancies between the experimental and calculated values of the $I(\hbar\omega)$ function [Fig. 4(a)] indicated that the pairing fields in ^{123}Xe are smaller than the ones in ^{124}Xe and ^{128}Ba, which is expected for odd-mass nuclei.

A better agreement is achieved between experimental and theoretical values of ratios of the reduced transition probabilities for the $\pi[h_{11/2}(d_{5/2}/g_{7/2})]\otimes\nu[h^2_{11/2}(d_{5/2}/g_{7/2})]$ configuration [see Fig. 4(b)]. The calculated $B(M1)/B(E2)$ ratios for this configuration reproduce the strongly decreasing trend of the experimental $B(M1)/B(E2)$ values, while the calculation for the $\pi[h_{11/2}(d_{5/2}/g_{7/2})]\otimes\nu[h_{11/2}(d_{5/2}/g_{7/2})d_{3/2}]$ configuration cannot reproduce the trend and the discrepancy with the experimental values is much larger. These results are consistent with the observed decay of band T (Fig. 1) and the behavior of the alignment as a function of rotational frequency (Fig. 3). As discussed above, the initial alignment of the $\pi[h_{11/2}(d_{5/2}/g_{7/2})]\otimes\nu[h_{11/2}(d_{5/2}/g_{7/2})d_{3/2}]$ configuration would be $i_x\approx6\hbar$ (the same as for the $\pi[h_{11/2}(d_{5/2}/g_{7/2})]\otimes\nu[h_{11/2}(d_{5/2}/g_{7/2})]$ configuration in ^{124}Xe), which contradicts the experimental observations. If a perpendicular coupling of the spins of the valence protons and neutrons is assumed at the bottom of the band, the $\pi[h_{11/2}(d_{5/2}/g_{7/2})]\otimes\nu[h^2_{11/2}(d_{5/2}/g_{7/2})]$ configuration yields a value of $I=\frac{31}{2}^-$ for the spin parity of the bandhead. Based on these considerations $I^\pi=(\frac{31}{2}^-)$ was adopted for the spin parity of the first state which was observed in band T. The lengths of the spin vectors of the valence particles and holes are relatively different, which makes the shears arrangement unstable. This might be an explanation for the dipole band in ^{123}Xe being shorter than the one in ^{124}Xe. For comparison, a theoretical curve, which was obtained within the framework of the geometrical model [14] for the $\pi[h_{11/2}d_{5/2}]\otimes\nu[h^2_{11/2}g_{7/2}]$ configuration at prolate deformation, $\varepsilon_2=0.2$, is presented in Fig. 4(b). The following values were accepted in this calculation: the g factors for the different orbitals were taken from Ward *et al.* [8]. The K quantum number is approximately good for the γ-soft Xe nuclei and a value $K=9$ was assumed for the above configuration. The experimental alignment was distributed among the quasiparticles in the same way as in Ref. [12] and the observed difference of $3\hbar$ was attributed to the additional neutron in $h_{11/2}$ orbital. The trend of the experimental $B(M1)/B(E2)$ values cannot be described in this case. On the other hand, for the $\pi[h_{11/2}(d_{5/2}/g_{7/2})]\otimes\nu[h^2_{11/2}(d_{5/2}/g_{7/2})]$ configuration, which is obtained in the framework of the TAC model, the tilt angle [Fig. 5(b)] gradually increases from 63° at $\hbar\omega\approx100$ keV to 73° at $\hbar\omega\approx450$ keV and approaches the strong coupling limit faster than in the case of ^{124}Xe [see Fig. 5(a)]. Also in this case, as for the dipole band in ^{124}Xe, we interpret band T in ^{123}Xe as a dipole band of intermediate character.

IV. CONCLUSIONS

In summary, we have observed a new $\Delta I=1$ band in^{123}Xe. This band and the similar dipole band in^{124}Xe are interpreted in the framework of the TAC model $5qp$ and $4qp$ magnetic bands of intermediate character, respectively. Concerning the calculated moments of inertia of these bands only a poor agreement is obtained which could be, however, improved by a fine tuning of the pairing properties. The observed trends of the measured $B(M1)/B(E2)$ ratios are described by the calculations when selecting the tilted configurations in which both the $h_{11/2}$ proton and $h_{11/2}$ neutrons are occupied. Thus, in combination with the results of Ref. [16] for ^{128}Ba a consistent description of the $M1/E2$ decay properties in the $A\approx130$ mass region based on tilted bands is obtained. The calculations suggest that both the shears mechanism and the collective rotation contribute to the generation of the the angular momentum in these bands indicating that this is a structural feature of the nuclei in this region.

ACKNOWLEDGMENTS

The authors are grateful to Dr. C. W. Beausang and Dr. E. S. Paul for reading and commenting on the manuscript. G.R. acknowledges support from FZ Rossendorf, by the DAAD under Contract No. A/99/08058, and an I.N.F.N. grant at the University of Camerino.

[1] S. Frauendorf, Nucl. Phys. **A557**, 259c (1997).

[2] R.M. Clark and A. Macchiavelli, Annu. Rev. Nucl. Part. Sci. **50**, 1 (2000).

[3] Amita, A.K. Jain, and B. Singh, At. Data Nucl. Data Tables **74**, 283 (2000).

[4] S. Frauendorf, Z. Phys. A **385**, 163 (1993).

[5] S. Frauendorf, Rev. Mod. Phys. **73**, 463 (2001).

[6] V.I. Dimitrov, S. Frauendorf, and F. Dönau, Phys. Rev. Lett. **84**, 5732 (2000).

[7] R. Wyss, in *Proceedings of the XXV International Winter Meeting on Nuclear Physics*, Bormio, 1987, edited by I. Iori, University Milano, Ricerca Scientifica ed Educacione Permanente, Supplemento No. 56, 1987, p. 542.

[8] D. Ward *et al.*, Nucl. Phys. **A529**, 315 (1991).

[9] O. Vogel *et al.*, Eur. Phys. J. A **4**, 323 (1999); I. Wiedenhöver *et al.*, Phys. Rev. C **58**, 721 (1998); O. Vogel *et al.*, *ibid.* **56**, 1338 (1997).

[10] F. Seiffert, W. Lieberz, A. Dewald, S. Freund, A. Gelberg, A. Granderath, D. Lieberz, R. Wirowski, and P. von Brentano, Nucl. Phys. **A554**, 287 (1993).

[11] G. Lo Bianco, Ch. Protochristov, G. Falconi, N. Blasi, D. Bazzacco, G. de Angelis, D.R. Napoli, M.A. Cardona, A.J. Kreiner, and H. Somacal, Z. Phys. A **359**, 347 (1997).

[12] I. Schneider *et al.*, Phys. Rev. C **60**, 014312 (1999).

[13] M. Serris *et al.*, Z. Phys. A **358**, 37 (1997).

[14] F. Dönau and S. Frauendorf, in *Proceedings of the Conference on High Angular Momentum Properties of Nuclei*, Oak Ridge, 1982, edited by N.R. Johnson (Harwood Academic, New York, 1982), p. 143; F. Dönau, Nucl. Phys. **A471**, 469 (1987).

[15] P. Petkov *et al.*, Phys. Rev. C **62**, 014314 (2000); P. Petkov *et al.*, Nucl. Phys. **A640**, 293 (1998).

[16] V.I. Dimitrov, F. Dönau, and S. Frauendorf, Phys. Rev. C **62**, 024315 (2000).

[17] D. Bazzacco, Proceedings of the International Conference on Nuclear Structure at High Angular Momentum, Ottawa, 1992 Chalk River Report (AECL 10613), p. 386.

[18] K.S. Krane, R.M. Steffen, and R.M. Wheeler, Nucl. Data Tables **11**, 351 (1973).

[19] A. Krämer-Flecken, T. Morek, R.M. Lieder, W. Gast, G. Hebbinghaus, H.M. Jager, and W. Urban, Nucl. Instrum. Methods Phys. Res. A **275**, 333 (1989).

[20] A. Schmidt *et al.*, Eur. Phys. J. A **2**, 21 (1998).

[21] S. Cwiok, J. Dudek, W. Nazarewicz, J. Nyberg, and K. Schiffer, Comput. Phys. Commun. **46**, 379 (1987).

[22] R. Wyss *et al.*, Nucl. Phys. **A505**, 337 (1989).